γ-ray spectroscopy of fission fragments produced in ^{208}Pb(^{18}O,f)

P. Banerjee,[1] S. Ganguly,[2] M. K. Pradhan,[1] Md. Moin Shaikh,[1] H. P. Sharma,[3] S. Chakraborty,[3] R. Palit,[4] R. G. Pillay,[4] V. Nanal,[4] S. Saha,[4] J. Sethi,[4] and D. C. Biswas[5]

[1]*Saha Institute of Nuclear Physics, Sector 1, Block AF, Bidhan Nagar, Kolkata 700 064, India*

[2]*Department of Physics, Bethune College, Kolkata 700 006, India*

[3]*Benaras Hindu University, Varanasi 221005, India*

[4]*Tata Institute of Fundamental Research, Mumbai 400 005, India*

[5]*Bhabha Atomic Research Centre, Anushaktinagar, Mumbai 400 085, India*

(Received 23 February 2015; revised manuscript received 24 June 2015; published 24 August 2015)

Prompt gamma-ray spectroscopy of fission fragments produced in the heavy-ion induced fusion-fission reaction ^{208}Pb(^{18}O, f) at $E = 90$ MeV has been performed. The relative isotopic yields of the fission fragments and the fragment mass distribution have been studied. Structures in the mass distribution have been discussed in the light of earlier results. Relative yields of several odd-A isotopes of Mo, Ru, Pd, and Cd and the odd-A isotones with $N = 62$ and 64 have been studied along with the yields of the neighboring even-Z, even-N fragments and correlated to nuclear structural effects. The average total neutron multiplicity during fission has been measured to be 5.48±0.59. The level schemes of the two neutron-rich nuclei ^{110}Pd and ^{116}Cd have been studied from γ-ray triple coincidence data. A large number of transitions, previously reported only from β-decay studies, have been observed in ^{110}Pd for the first time. The yrast band in ^{116}Cd has been extended up to spin (16^+). In addition, a rotational sequence built upon an excited 5^- state in ^{116}Cd has been observed up to (13^-). The level schemes have been discussed in the context of existing results, both experimental and theoretical, in the literature.

DOI: 10.1103/PhysRevC.92.024318 PACS number(s): 25.85.Ge, 24.75.+i, 27.60.+j, 23.20.Lv

I. INTRODUCTION

Primary fission fragments produced in heavy-ion- (HI) induced fusion-fission reactions have a neutron/proton ratio that is similar to that of the fissioning system and thus lie on the neutron-rich side of the β stability line. Prompt γ-ray spectroscopy of such fission fragments has therefore been widely used in recent years for studying the structure of neutron-rich nuclei near the line of stability. Although cold spontaneous fission can produce relatively more neutron-rich nuclei [1], fusion-fission reactions are favored because of their larger excitation energy leading to a broader mass distribution and larger values of fragment spin [2]. The study of the mass distributions provides information about the fission mechanism, shape evolution of the fissioning nucleus, and nuclear shell closures. The prompt γ rays emitted by the fragments are also an important source of information regarding nuclear excitation energy, spin, and structure of the fission fragments.

The present work relates to the spectroscopic study of prompt γ rays emitted by fission fragments produced in the HI-induced fusion-fission reaction ^{208}Pb(^{18}O, f) at $E = 90$ MeV. Total intensities of the transitions feeding into the ground state of a fission fragment represent the total independent yield of that fragment. The relative yields of the different fission fragments following the emission of prompt neutrons, extracted primarily from threefold γ-ray coincidence data, is a direct measure of the fragment mass distribution. A general feature of such mass distribution is that the yields of the even-even nuclides are enhanced relative to the even-odd ones due to the stabilization effect of nucleon pairing. In addition, nuclear structure effects are manifest in the fragment yield. Closed-shell nuclei are known to have a significantly lower yield [3,4]. A study of some even-even and odd-A nuclei has been undertaken in the present work in order to gain an insight into the structure of such nuclei. The other areas of interest in the present work include the study of the level schemes of neutron-rich nuclei with $A \sim 110$ and the extent of population of the high spin states in these nuclei. While highly neutron-rich nuclei in this mass region have been reported to be well populated in spontaneous fission of ^{248}Cm and ^{252}Cf [5,6], the relatively less neutron-rich ones such as those near the line of stability have been studied from heavy-ion induced fission [7]. Neutron-rich nuclei have also been studied from deep-inelastic reactions and β decay. The level schemes of the two neutron-rich nuclei ^{110}Pd and ^{116}Cd, both fairly well populated in the reaction ^{208}Pb(^{18}O, f), have been studied in the present work using $\gamma\gamma\gamma$-coincidence data in an attempt to look for new information on the spectroscopic study of their level structures.

II. EXPERIMENTAL METHOD

The experiment was performed using a 90-MeV ^{18}O beam, with a beam current of about 1.5 pnA, on a self-supporting 30-mg/cm^2 enriched (99.3%) ^{208}Pb foil at the BARC-TIFR Pelletron LINAC facility at Mumbai, India. The cross section of the fusion-fission reaction ^{208}Pb(^{18}O, f) is about 270 mb at 90 MeV and the Coulomb barrier for the reaction is 76 MeV (obtained using the code PACE4). The excitation energy of the compound nucleus ^{226}Th is approximately 37 MeV. With a beam energy loss of about 1.6 MeV cm^2/mg in ^{208}Pb, most of the reactions occurred within the first 25–30% thickness of the target and almost all fission fragments produced were stopped within the target, requiring no Doppler shift correction. The γ rays from the fission fragments were detected using the Indian National Gamma Array (INGA) comprising 20 Compton-suppressed clover HPGe detectors.

Nine of the detectors were located in the backward hemisphere, seven in the forward hemisphere, and four at 90° with respect to the beam direction. Three- and higher-fold coincidence events were recorded in a fast digital data acquisition system based on Pixie-16 modules of XIA LLC [8]. The data were sorted to generate symmetric $\gamma\gamma$ matrices and $\gamma\gamma\gamma$ cubes which were subsequently analyzed using the software package RADWARE [9]. About 2.9×10^8 threefold events were available for analysis.

The relative yields of the even-Z, even-N fragments produced in the fission of the compound system ^{226}Th were determined mostly from the intensity of the $2^+ \rightarrow 0^+$ transition in the sum of the spectra gated by the transition(s) feeding the 2^+ state. In some cases, as in ^{100}Mo, intensities of transitions other than the $2^+ \rightarrow 0^+$ transition that have a significant feeding into the ground state were also included in determining the yield. In addition, the contribution of long-lived isomers to the yield, as in $^{120-126}$Sn, that did not decay significantly to the lower-lying states, were considered. This was done by estimating the population of the isomeric states from gates set on transitions above the isomer. Spurious contribution due to contamination peaks in the gated spectra were carefully looked into and corrected for in all cases.

Moreover, the relative yields for several odd-A isotopes of Mo, Ru, Pd, and Cd and the odd-A isotones of $N = 62$ and 64 have also been measured in the present work. Such data are relatively scarce since detailed spectroscopic data are not available for many odd-A nuclei in the literature. Also, the presence of multiple low-energy isomeric states with long half-lives in some odd-A nuclei (viz. ^{101}Mo) renders the yield determination a relatively complex exercise. However, although multiple isomeric states are previously reported in some odd-A nuclei, not all such states were populated in the present experiment. For example, in ^{101}Mo, only one isomeric state at 273 keV with $T_{1/2} = 105(8)$ ns of the three previously reported isomers [10,11] was populated. Similarly, only the 21-keV isomeric state with $T_{1/2} = 340(15)$ ns was observed in ^{105}Ru (from the observation of the 445-keV transition that feeds this state) although several low-energy isomers are reported in the literature [12]. The observed decays from these isomeric states are strongly reduced since their half-lives are comparable to the time window (200 ns) used in the present experiment. Also, the 209-keV $11/2^-$ state in ^{105}Ru has not been previously observed to decay to any of the lower-lying states, suggesting that the state is a long-lived isomer [13]. Hence, the population of this state has been included in determining the yield of ^{105}Ru. However, the fragment mass distribution for odd-A isotopes could be determined reliably only for a few nuclei in the present work where the yields are relatively large and the intensities of all relevant transitions could be measured with sufficient accuracy.

The cross sections for the emission of light charged particles like proton and α particles is insignificant (about 1%) compared to neutron emission cross sections from the fission of the compound nucleus ^{226}Th, produced in $^{208}\mathrm{Pb} + {}^{18}\mathrm{O}$ at $E =$ 90 MeV. Thus, the sum of the charges of the two correlated fragments is assumed to be the same as the charge of the compound nucleus $Z = 90$. The correlated yield distribution in Fig. 1 shows that the five to six neutron emission channels

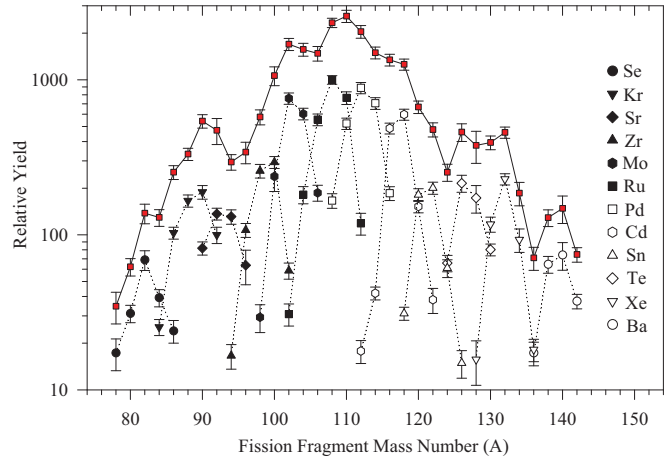

FIG. 1. (Color online) Relative fission fragment isotopic distribution for 12 even-Z, even-N fragments from the reaction $^{208}\mathrm{Pb}(^{18}\mathrm{O}, f)$ at $E = 90$ MeV. Each complementary pair is represented by the same symbol with the light fragment shown by a filled symbol and the heavy fragment using an open symbol. The data points are joined by broken lines. The fission-fragment mass distribution, obtained by summing the yields of the individual nuclei having the same mass number, multiplied by 2, is shown at the top. These data points are connected by a continuous line.

dominate. Plots of the relative yields of some odd-A isotopes of Mo, Ru, Pd and Cd and the odd-A isotones of $N = 62$ and 64 are shown in Fig. 2. The relative yields of the different fragments (corresponding to different neutron multiplicities), obtained from a spectrum gated on the $2^+ \rightarrow 0^+$ transition of a correlated fragment, has been used to provide an estimate of the neutron multiplicity. The results are plotted in Fig. 3 and discussed in the next section.

Level schemes of the two neutron-rich nuclei ^{110}Pd and ^{116}Cd have been studied in the present work from $\gamma\gamma\gamma$-coincidence data. The γ-ray relative intensities were determined from double-gated spectra with one gate on the $2^+ \rightarrow 0^+$ transition in the primary nucleus of interest (^{110}Pd and ^{116}Cd in this case) and the second gate on the strong lower-lying transitions of the yrast band in the complementary fragment. This spectrum permits the determination of the relative intensities of all transitions in the primary nucleus except the $2^+ \rightarrow 0^+$ transition and eliminates the contribution of β decay to the intensities of the γ rays measured in the experiment. For ^{110}Pd, the double-gated spectrum consisted of the sum of two spectra in each of which one gate was set on the 373.7 keV, $2^+ \rightarrow 0^+$ transition in ^{110}Pd and the other gate was set successively on the 241 keV, $2^+ \rightarrow 0^+$ transition and the 422 keV, $4^+ \rightarrow 2^+$ transition in the complementary ^{108,110}Ru isotopes, corresponding to eight and six neutron emission channels, respectively. It may be noted that the $2^+ \rightarrow 0^+$ and $4^+ \rightarrow 2^+$ transitions have almost identical energies in ^{108,110}Ru. For ^{116}Cd, three such double-gated spectra were added to improve the data statistics. Here the first gate was set on the 513.3-keV γ ray in ^{116}Cd and the second gate was set successively on the three lowest $2^+ \rightarrow 0^+$, $4^+ \rightarrow 2^+$, and the $6^+ \rightarrow 4^+$ transitions in the complementary fragment ^{104}Mo. The resulting sum of the three double-gated spectra is shown in

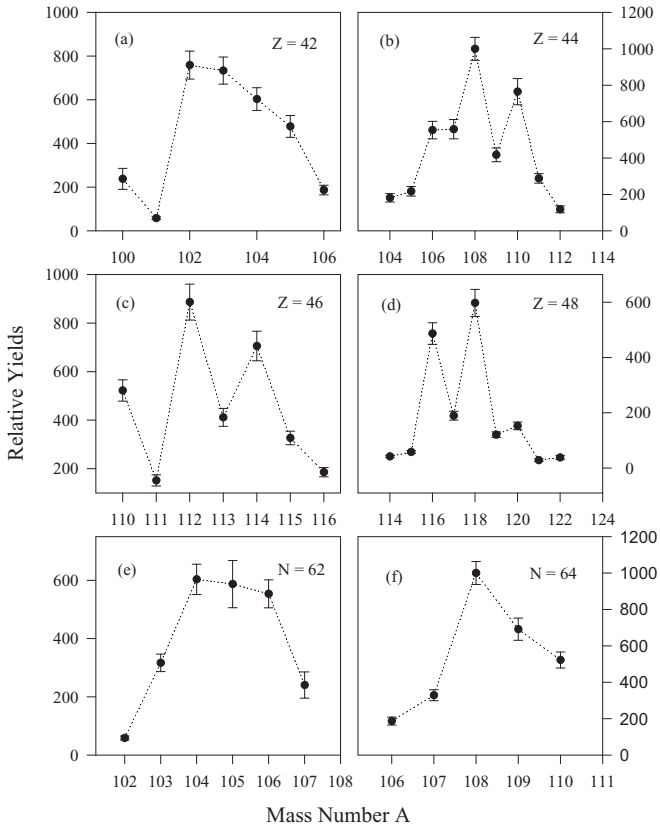

FIG. 2. The plots in (a)–(d) show the relative yields of the odd- and even-A isotopes of Mo ($Z = 42$), Ru ($Z = 44$), Pd ($A = 46$), and Cd ($Z = 48$) plotted as a function of A. Plots (e) and (f) show the relative yields of the isotones with $N = 62$ and 64, respectively.

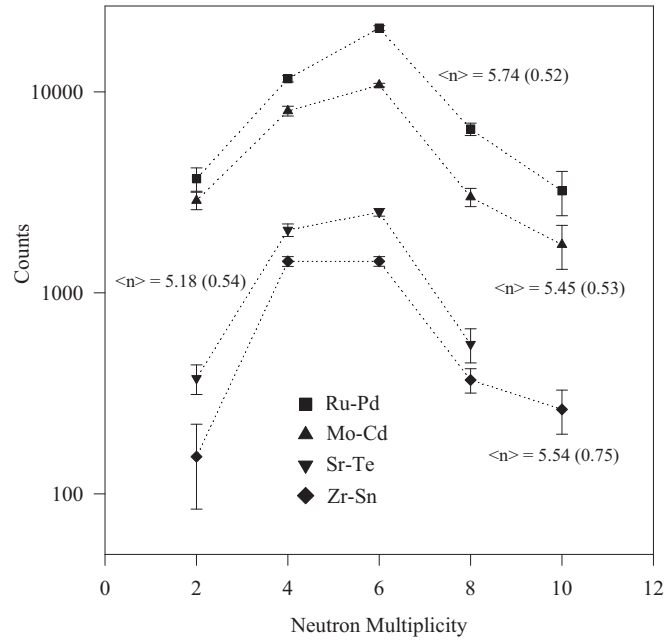

FIG. 3. The total pre- and postscission neutron multiplicities per fission event for four pair of complementary fragments Sr-Te, Zr-Sn, Mo-Cd, and Ru-Pd obtained in the present work.

Fig. 4. Most of the transitions belonging to ^{116}Cd can be seen in this spectrum except the weak 265.2-, 509.0-, and 931.6-keV γ rays. Relative intensities for these transitions were determined as outlined below in Sec. III B. Generally, for all transitions near the top of the band where the states are populated only from prompt high-spin fission decay, the relative intensities were measured using spectra with both gates set on transitions in the primary nucleus. These intensities were then normalized with the intensity of at least one of the lower-lying transitions in the band that also has no contribution from β decay and was determined with one gate on a complementary fragment transition. Finally, the intensity of the $2^+ \rightarrow 0^+$ transition relative to that of the $4^+ \rightarrow 2^+$ transition was estimated from spectra gated on the two lowest-lying transitions in the complementary fragment. Appropriate normalization was done so that the relative intensities are obtained with respect to 100 for the $4^+ \rightarrow 2^+$ transition. Further details are given in Sec. III B.

III. EXPERIMENTAL RESULTS AND DISCUSSION

The relative isotopic yields of 12 even-A (even-Z, even-N) isotopes belonging to complementary charge pairs, namely Se-Ba, Kr-Xe, Sr-Te, Zr-Sn, Mo-Cd, and Ru-Pd, have been determined in the present work. The resulting correlated fragment isotopic distribution, with the yields normalized to 1000 for the yield of the most strongly produced isotope ^{108}Ru, is shown in Fig. 1. The fragment mass distribution, obtained by summing the yields of individual nuclei with the same mass is also shown in the same figure. In addition, the relative yields for several odd-A isotopes of nuclei with $Z = 42$, 44, 46, and 48 and the odd-A isotones corresponding to $N = 62$ and 64 have been measured in the present work. The results are shown in Fig. 2. Such data are relatively scarce (compared to the even-even nuclei) in the literature, as already stated above. The average neutron multiplicities for four pairs of complementary fragments have been determined and plotted in Fig. 3. Lastly, the level schemes of two neutron-rich nuclei ^{110}Pd and ^{116}Cd have been studied. Partial level schemes of these two nuclei are shown in Figs. 5 and 6 and the corresponding gated spectra in support of the decay schemes are given in Figs. 7, 8, and 9. Tables I and II summarize the relative intensities of the γ rays in the two nuclei. The results have been discussed in the light of existing experimental and theoretical data in the following subsections.

A. *Fission-fragment distributions and neutron multiplicities*

The fission-fragment isotopic distribution for even-A isotopes obtained in the present work (Fig. 1) is expectedly quite similar with the distribution reported earlier [4], as both experiments employ the same reaction at similar projectile energies ($E = 90$ MeV in the present work as compared to 85 MeV in Ref. [4]). The postneutron emission isotopic yield distributions are narrow, with only four to six isotopes observed for each Z value having significant yields. The yields of the Sn isotopes, as expected, are somewhat small due to the effect of the $Z = 50$ shell closure (discussed below). The yields of the

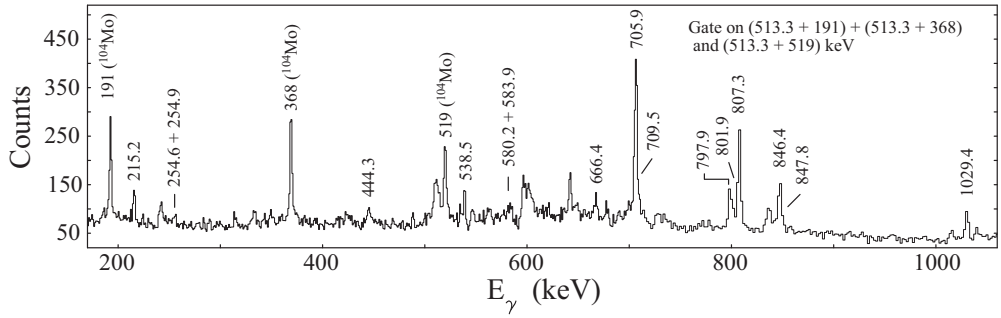

FIG. 4. Sum of double-gated spectra with gates on (513.3 + 191), (513.3 + 368), and (513.3 + 519) keV where the 513.3-keV γ ray belongs to ^{116}Cd and the 191-, 368-, and 519-keV γ-rays belong to ^{104}Mo.

corresponding complementary fragments with $Z = 40$ (i.e., the Zr isotopes) are also similarly small. Interestingly, the Sr isotopes ($Z = 38$) have significantly smaller yields compared to even the neighboring Kr ($Z = 36$) isotopes. It is possible that the low yields of $^{90-96}$Sr are related to the effect of subshell closures of low-j orbitals at $Z = 38$ and $N = 56$, leading to very low collectivity. Indeed, the $2^+ \rightarrow 0^+$ transitions in the three even-even $^{90-94}$Sr nuclei are all reported to have low $B(E2)$ values in the range 8–13 W.u. [14].

The fission-fragment mass distribution, obtained by summing the yields of the individual nuclei having the same mass number, is also shown at the top of Fig. 1. The distribution, multiplied by a factor 2, is plotted and joined by a continuous line in the figure. The mass distribution is symmetric about $A = 110$. This is almost equal to half the mass of the compound nucleus ^{226}Th, the difference being due to the mass of the neutrons emitted in the fusion-fission process. Fission fragment mass distribution obtained from the reaction ^{208}Pb(^{18}O, f) at 85 MeV and spanning the same mass region as in the present work has been previously reported by Bogachev *et al.* [4] while Danu *et al.* [3] have reported the mass distribution for the reaction ^{238}U(^{18}O, f) at 100 MeV for masses in the range $A = 90$–158 a.m.u. All three mass distributions (including the present one) show structures that are related to the nuclear shell effects and nuclear structure. The present fragment mass distribution (Fig. 1) shows dips at $A = 94$–96, 124, and 136. In addition, the distribution tends to drop at $A = 84$. There is a general agreement of this distribution with those reported earlier [3,4]. The mass distribution reported in Ref. [3] shows clear minima at $A = 124$ and 136 and a somewhat shallow minimum at $A = 112$. The distribution reported by Bogachev *et al.* [4] shows prominent minima at $A = 96$–98, 124, and 136 and a somewhat smaller dip at $A = 84$.

Fission fragment mass distribution is known to show structures with dips in the distribution arising primarily due to shell closure of one of the two fragments. During the transition from the saddle to the scission point, with the fissioning nucleus evolving into an elongated shape, the contribution to fission is reduced if one of the fission partners has a closed-shell configuration. The closed-shell partner resists deformation and its complementary fragment has to attain a large deformation in the saddle-to-scission dynamics. This results in a decrease in the yield corresponding to these fission partners. As explained

TABLE I. Present experimental results on level energies (E_x), γ-ray energies (E_γ) and γ-ray relative intensities (with errors given within parentheses) for ^{110}Pd. J_i^π and J_f^π refer to the spin and parity of the initial and final states, respectively.

Band	E_x (keV)	E_γ (keV)	Relative Intensities	$J_i^\pi \rightarrow J_f^\pi$	Band	E_x (keV)	E_γ (keV)	Relative Intensities	$J_i^\pi \rightarrow J_f^\pi$
Band 1	373.7	373.7	170.9 (19.1)	$2_1^+ \rightarrow 0^+$	Other states	1900.1	502.1	1.8[a]	$(5_1^+) \rightarrow (4_2^+)$
	921.2	547.5	100 (7.5)	$4_1^+ \rightarrow 2_1^+$			688.1	16.1 (4.1)	$(5_1^+) \rightarrow (3^+)$
	1574.5	653.3	72.9 (7.6)	$6_1^+ \rightarrow 4_1^+$			978.9	1.6[a]	$(5_1^+) \rightarrow 4_1^+$
	2296.5	722.0	20.0 (4.5)	$(8_1^+) \rightarrow 6_1^+$			1086.1	3.5[a]	$(5_1^+) \rightarrow (2_2^+)$
	3070.8	774.3	8.0 (2.7)	$(10^+) \rightarrow (8_1^+)$		2261.2	1049.2	6.8 (2.7)	$(5_2^+) \rightarrow (3^+)$
	3720.2	649.4	5.7 (2.1)	$(12^+) \rightarrow (10^+)$			1340.0	2.5[a]	$(5_2^+) \rightarrow 4_1^+$
	4487.3	767.1	5.1 (1.9)	$(14^+) \rightarrow (12^+)$		2791.4	891.3	8.1 (2.9)	$(6_3^+) \rightarrow (5_1^+)$
Band 2	814.1	440.4	36.4 (4.9)	$2_2^+ \rightarrow 2_1^+$			1216.9	1.8[a]	$(6_3^+) \rightarrow 6_1^+$
		814.1	13.8 (3.0)	$2_2^+ \rightarrow 0^+$			1393.3	4.7 (2.0)	$(6_3^+) \rightarrow (4_2^+)$
	1212.0	290.7	1.9[a]	$(3^+) \rightarrow 4_1^+$			1579.4	~1[a]	$(6_3^+) \rightarrow (3^+)$
		397.9	16.4 (3.7)	$(3^+) \rightarrow 2_2^+$		2805.2	544.1	5.6 (2.3)	$(6_4^+) \rightarrow (5_2^+)$
		838.3	22.6 (5.6)	$(3^+) \rightarrow 2_1^+$			818.1	1.4[a]	$(6_4^+) \rightarrow (6_2^+)$
	1398.1	476.7	9.5 (3.1)	$4_2^+ \rightarrow 4_1^+$			905.1	13.5 (3.2)	$(6_4^+) \rightarrow (5_1^+)$
		584.0	18.7 (4.4)	$4_2^+ \rightarrow 2_2^+$			1230.7	6.6 (2.7)	$(6_4^+) \rightarrow 6_1^+$
	1987.1	589.0	7.1 (2.4)	$(6_2^+) \rightarrow (4_2^+)$			1407.1	5.0 (2.6)	$(6_4^+) \rightarrow (4_2^+)$
	2651.1	664	~2	$(8_2^+) \rightarrow (6_2^+)$			1593.2	2.8[a]	$(6_4^+) \rightarrow (3^+)$

[a]Relative intensities determined from previous branching ratios [24].

TABLE II. Present experimental results on level energies (E_x), γ-ray energies (E_γ), and γ-ray relative intensities (with errors given within parentheses) for ^{116}Cd. J_i^π and J_f^π refer to the spin and parity of the initial and final state respectively.

Nucleus	Band	E_x (keV)	E_γ (keV)	Relative intensities	$J_i^\pi \rightarrow J_f^\pi$
^{116}Cd	Band 1	513.3	513.3	103.5 (9.8)	$2^+ \rightarrow 0^+$
		1219.2	705.9	100 (6.8)	$4^+ \rightarrow 2^+$
		2026.5	807.3	65.8 (6.4)	$6^+ \rightarrow 4^+$
		2824.4	797.9	25.7 (3.7)	$8_1^+ \rightarrow 6^+$
		3039.6	166.7	5.3 (2.0)	$10^+ \rightarrow 8_2^+$
			215.2	16.8 (3.0)	$10^+ \rightarrow 8_1^+$
		3578.1	538.5	17.3 (3.1)	$12^+ \rightarrow 10^+$
		4380.0	801.9	13.1 (5.2)	$(14^+) \rightarrow 12^+$
		5227.8	847.8	6.6 (2.4)	$(16^+) \rightarrow (14^+)$
	Band 2	2248.6	1029.4	24.4 (4.3)	$5_1^- \rightarrow 4^+$
		2692.9	444.3	6.1 (2.1)	$(7_1^-) \rightarrow 5_1^-$
			666.4	13.6 (3.2)	$(7_1^-) \rightarrow 6^+$
		2958.1	265.2	2.7 (1.2)	$(6_2^-) \rightarrow (7_1^-)$
			709.5	9.4 (3.0)	$(6_2^-) \rightarrow 5_1^-$
			931.6	2.0 (1.3)	$(6_2^-) \rightarrow 6^+$
		3212.7	254.6	6.9 (1.9)[a]	$- \rightarrow (6_2^-)$
		3238.6	545.7	10.5 (2.4)	$(9^-) \rightarrow (7_1^-)$
		3721.7	509.0	~3	—
		3915.5	676.9	7.3 (2.0)	$(11^-) \rightarrow (9^-)$
		4604.7	689.2	5.8 (1.9)	$(13^-) \rightarrow (11^-)$
	Other states	2503.5	254.9	6.9 (1.9)[a]	$5_2^- \rightarrow 5_1^-$
		2828.8	580.2	5.7 (3.4)	$(6_1^-) \rightarrow 5_1^-$
		2872.9	846.4	17.5 (4.3)	$8_2^+ \rightarrow 6^+$
		3087.4	583.9	~1	$(7_2^-) \rightarrow 5_2^-$

[a]Combined relative intensity for 254.6- and 254.9-keV γ rays.

earlier [3], the dips in the mass distribution at $A = 124$ is due to the influence of the $Z = 50$ closed shell and that at $A = 136$ is because of the $N = 82$ closed shell. The minima in the distribution corresponding to the complementary fission partners should occur at $A = 84$ and 96, considering that the average number of neutrons emitted in the fusion-fission process is almost six (discussed below). The present results are in general agreement with these observations.

As stated earlier, the relative yields for several odd-A fragments have also been measured in the present work. The relative yields of both the odd- and even-A isotopes of Mo ($Z = 42$), Ru ($Z = 44$), Pd ($Z = 46$), and Cd ($Z = 48$) are plotted as a function of A in Figs. 2(a)–2(d). Also, the relative yields of the odd-A isotones with $N = 62$ and 64 are shown in Figs. 2(e) and 2(f) along with the yields of the neighboring even-even fragments. Measurements were made only for strongly populated odd-A fragments in which the yields from the cascades populating the ground state could be correctly estimated. Odd-even effects, a prominent structural feature observed in fission, with an enhanced production of even-Z, even-N fragments compared to the odd-A ones, superimposed on the gross shape of the yields, can be clearly seen for the $Z = 44$, 46 and 48 [Figs. 2(b)–2(d)] isotopes and the $N = 64$ [Fig. 2(f)] isotones. The effect is relatively small for the $Z = 42$ isotopes [Fig. 2(a)] and the $N = 62$ isotones [Fig. 2(e)]. It is also evident from Figs. 2(a)–2(d) that the odd-even effect in neutron number is more pronounced than the odd-even effect in proton number [Figs. 2(e) and 2(f)]. Neutron evaporation from the fragments following scission, facilitated by their large excitation energy, gives rise to a significant excess of even-Z, even-N fragments over the even-Z, odd-N species. Since evaporation of protons is relatively suppressed, the odd-even effect in proton number is comparatively small.

Apparently, the yields for the odd-A ^{103}Mo [Fig. 2(a)] and ^{105}Tc [Fig. 2(e)] are large and comparable to those for the neighboring even-A fragments. It may be noted that the nucleus ^{103}Mo belongs to the region of deformed neutron-rich nuclei in the $A = 100$ mass region. The quadrupole deformation of the first excited state at 102.6 keV (spin $5/2^+$) in ^{103}Mo is reported to be $\beta_2 = 0.34(1)$ [15]. For ^{105}Tc, triaxial-rotor-plus-particle model calculations have been previously found to be compatible with large deformation and triaxiality [16]. These findings are in general agreement with the observation that neutron-rich nuclei with N close to 60 are strongly deformed. The large relative yields of ^{103}Mo and ^{105}Tc, observed in the present work, are presumably related to their large deformations.

The average neutron multiplicities for four pairs of complementary fragments Sr-Te, Zr-Sn, Mo-Cd, and Ru-Pd have been determined in this work and plotted in Fig. 3. The average total number of neutrons emitted considering all four pairs is 5.48±0.59 and is similar to the result reported in Ref. [4]. These multiplicities represent the average number of neutrons emitted per fission event during the pre- as well as the postscission stages of the decay of the compound nucleus ^{226}Th. However, it is the postscission neutron multiplicities that are related to the fragment excitation energies and their shapes at scission. Larger postscission neutron multiplicities are associated with higher excitation energies of the fragments and larger fragment deformation. Information of postscission neutron multiplicities are obtained from fragment-neutron angular correlation measurements [17]. Assuming a prescission neutron multiplicity of about 3 [17], the postscission multiplicity is approximately 2.5 in the present work. This is expected to correspond to a moderate deformation of the fragments at scission [18].

B. *Level schemes*

The level schemes of the two neutron-rich nuclei ^{110}Pd and ^{116}Cd have been investigated in the present work. The relevant level schemes and the triple-γ coincident spectra that support the placement of the γ rays in the level schemes are discussed in the following subsections. All double-gated spectra presented in the paper are corrected for γ-ray relative efficiencies. The relative intensities of the transitions in the two nuclei from prompt fission decay are summarized in Tables I and II. Spin-parity assignments are based on earlier studies unless indicated otherwise.

1. *The nucleus* ^{110}Pd

The neutron-deficient Pd isotopes are good examples of vibrational nuclei while the neutron-rich ones exhibit behavior characteristic of a γ-soft rotor. The values of the energy

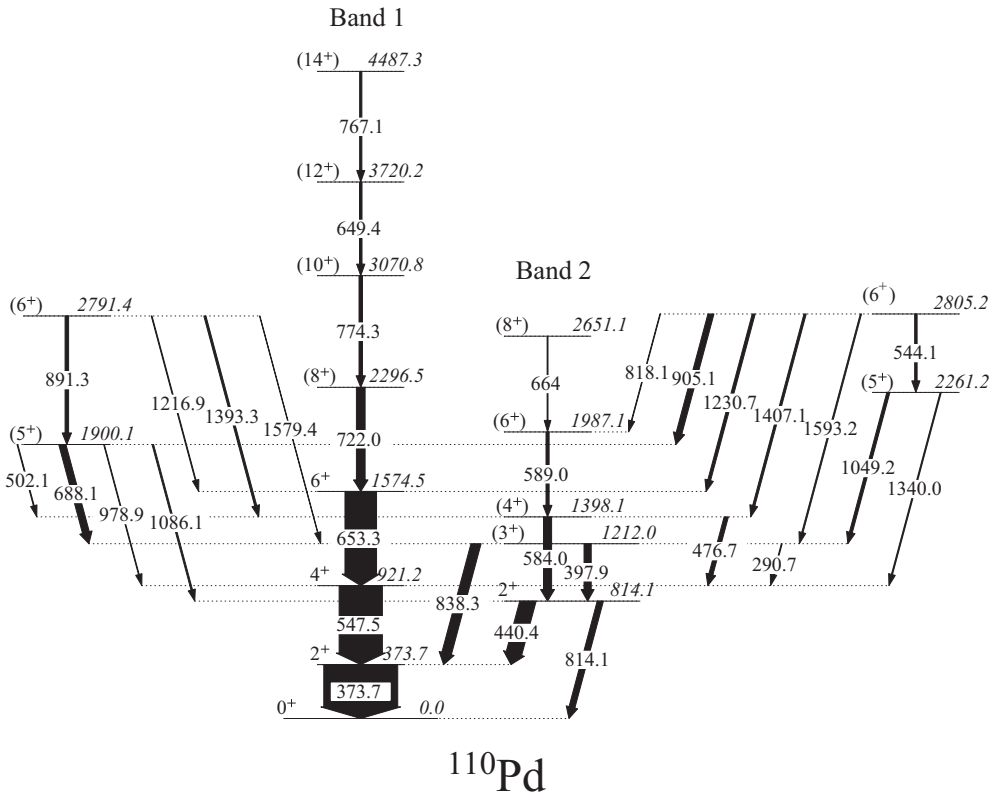

FIG. 5. Partial level scheme of ^{110}Pd obtained from the present experiment. The level and γ-ray energies are in keV. The relative intensities of the transitions are represented by the widths of the arrows.

ratio $E4^+/E2^+ = 2.4$–2.6, observed for $^{108-114}$Pd, are typical for γ-soft rotors. The excitation energies of the 2^+ states belonging to the ground-state bands in the even-A palladium isotopes $^{106-116}$Pd decrease smoothly from 512 keV for ^{106}Pd to 332 keV for ^{114}Pd. This also suggests a gradual development from a vibration-like toward a rotation-like structure with the neutron number N approaching the midshell region between $N = 50$ and $N = 82$. Indeed, the two $N = 64$ isotones ^{108}Ru and ^{110}Pd have the largest deformation of $\beta_2 = 0.28 \pm 0.01$ and 0.24 ± 0.01 in the $Z = 44$ and 46 chains, respectively [19]. However, the ground-state rotational bands in the neutron-rich even-mass palladium isotopes and ^{110}Cd have been reported to be crossed above spin 8^+ by a sequence of transitions having pure vibrational character. This indicates a coupling of vibrational and rotational motion. In addition, two-phonon γ-vibrational bands have also been reported in several neutron-rich even-A Pd isotopes, extending up to high spins such as (15^+) in ^{114,116}Pd.

The high-spin states of ^{110}Pd have been previously studied from the fusion-fission reactions ^{12}C + ^{238}U [20] and ^{31}P + ^{176}Yb [21]. The ground-state yrast band was observed up to spin 14^+ in these experiments. A detailed level scheme of ^{110}Pd up to an excitation energy of 2805 keV was also established from the β decay of the (6^+) isomeric state ($T_{1/2} = 28.0$ s) of ^{110}Rh [22,23]. Several states observed from the β-decay studies, including those belonging to the γ-vibrational band, were subsequently reported in Ref. [21].

The level scheme of ^{110}Pd obtained in the present work is shown in Fig. 5. Only the positive-parity states are shown. Negative-parity states were populated weakly and are not discussed here. Some of the states are grouped under two bands as shown in the figure. All levels in the ground-state band (Band 1) up to an excitation energy of 4487.3 keV and spin $J^\pi = (14^+)$, reported previously [20,21], were observed. The level spins are the same as those reported earlier [21]. Figure 7(a) shows the coincidence spectrum obtained from gating on the two lowermost transitions in the ground-state band. All γ rays in the band are seen in the spectrum, except the 649.4-keV γ ray, masked in the low-energy tail of the strong 653.3-keV γ ray, and the highest transition in the band with energy 767.1 keV. This last transition is weak and can be seen only in double-gated spectra (not shown) with at least one gate on a transition higher up in the band. States up to spin 6^+ and excitation energy 1574.5 keV in Band 1 have also been previously reported to be populated in the β decay of ^{110}Rh [22,23].

The other band (Band 2) is the γ band, observed up to an excitation energy of 2651.1 keV and spin (8^+) (see Fig. 5), as reported earlier [21]. The 2651.1-keV state, first reported in Ref. [21], was shown to decay by the 664-keV γ ray to the 1987.1-keV level. As seen from Fig. 7(b) in the present work, a reasonably strong 818.1-keV transition and a weaker 664-keV transition are observed in the spectra gated on the 373.7- and 584.0-keV transitions, suggesting that the 818.1-keV γ ray could also be a possible candidate for placement above the 1987.1-keV state. However, much of

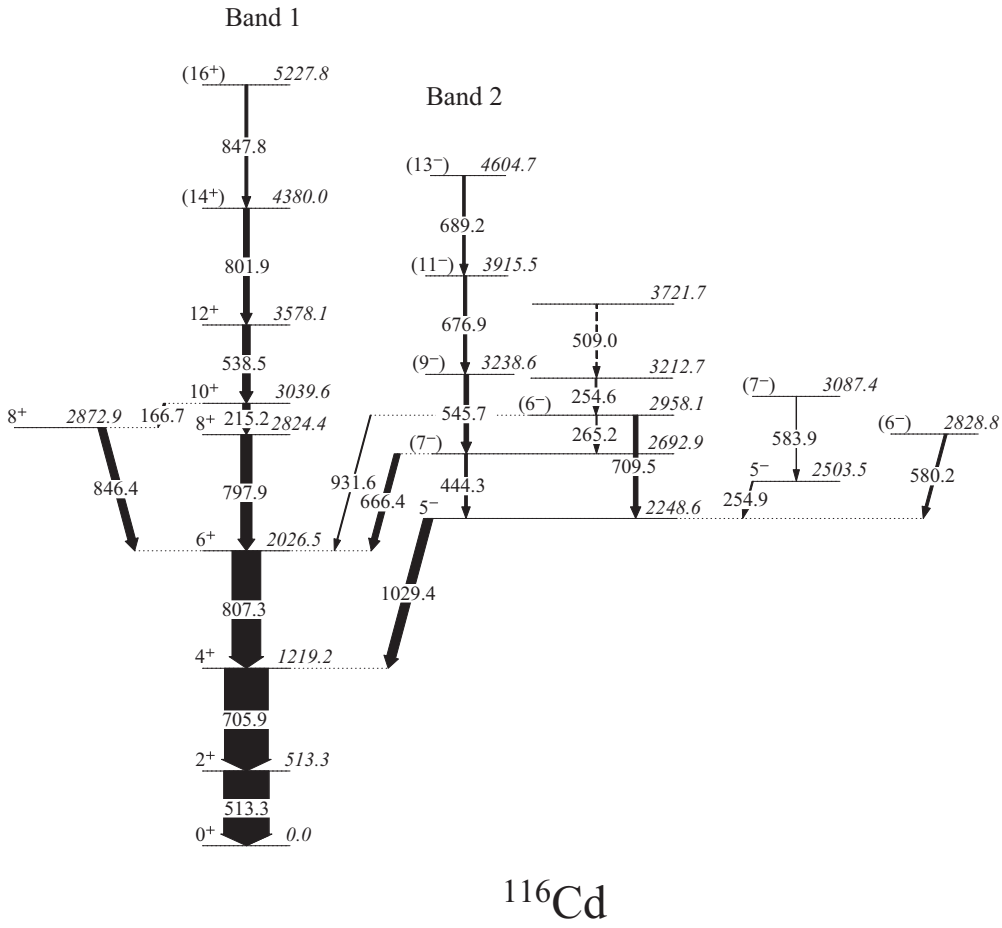

FIG. 6. Partial level scheme of ^{116}Cd based on the present work.

this intensity of the 818.1-keV γ ray, observed in Fig. 7(b), appears to come from the feeding to the 2805.2-keV state (Fig. 5) from the β decay of the 28.0 s isomer of ^{110}Rh [23], since the 818.1 transition is observed to be very weak in spectra with one gate on the complementary fragment ^{110}Rh. Hence, the 664-keV transition is placed at the top of Band 2, confirming the earlier assignment [21] of this transition in the level scheme. Moreover, the systematics of the level energies in the γ band in the neighboring even-even ^{108,112,114,116}Pd isotopes are consistent with the placement of the 664-keV γ ray in the band rather than the higher-energy 818.1-keV γ ray. The placement of the 818.1-keV γ ray in the level scheme, not reported in the earlier fission study [21], is consistent with the spectrum in Fig. 7(b) and the level scheme reported from the β decay of ^{110}Rh [23].

Furthermore, it may be noted that no evidence is found for the previously reported [21] 1759 keV, (5^+) state in Band 2 from the present data. The earlier reported $(5^+) \rightarrow (3^+)$, 547-keV transition from this level was stated to have a relative intensity similar to that of the 584.0-keV γ ray in Ref. [21]. Since the 584.0-keV transition is observed to be fairly strong with an intensity of 18.7 ± 4.4 relative to 100 for the $4^+ \rightarrow 2^+$, 547.5-keV transition (see Table I), it is plausible that the 547-keV γ ray from the previously reported (5^+) state should also have been observed in the present work. The spectrum gated by the 440.4- and 397.9-keV γ rays [inset of Fig. 7(b)] only shows a 544.1-keV γ ray depopulating the 2805.2-keV state (see Fig. 5). The expected position of the 547-keV transition is indicated with an arrow in this figure. Moreover, it may be noted that the 1759 keV, (5^+) state was also not reported from the β decay of the (6^+) isomeric state of ^{110}Rh, whereas all the four other states in the band with energies up to 1987.1 keV and spin (6^+) were observed. Based on these arguments, the (5^+) level, reported earlier [21], is not included in Band 2.

Beside Bands 1 and 2, four other states with energies 2261.2, 2805.2, 1900.1, and 2791.4 keV are observed in the present work that are strongly linked with the states of Bands 1 and 2 (Fig. 5). It may be noted that although most of the linking transitions are observed to have large intensities in the spectra in Fig. 7 and the inset therein (all of which have contributions from β decay also), only the stronger ones with relative intensities of about 5 units or more (see Table I) are clearly observed in spectra with one gate on the 373.7-keV transition in ^{110}Pd and the other gate on a complementary fragment transition. Evidently, this is due to limitations in data statistics. However, it also indicates that the 2261.2-, 2805.2-, 1900.1-, and 2791.4-keV states, mentioned above, are more strongly fed from β decay compared to prompt fission decay in the present experiment.

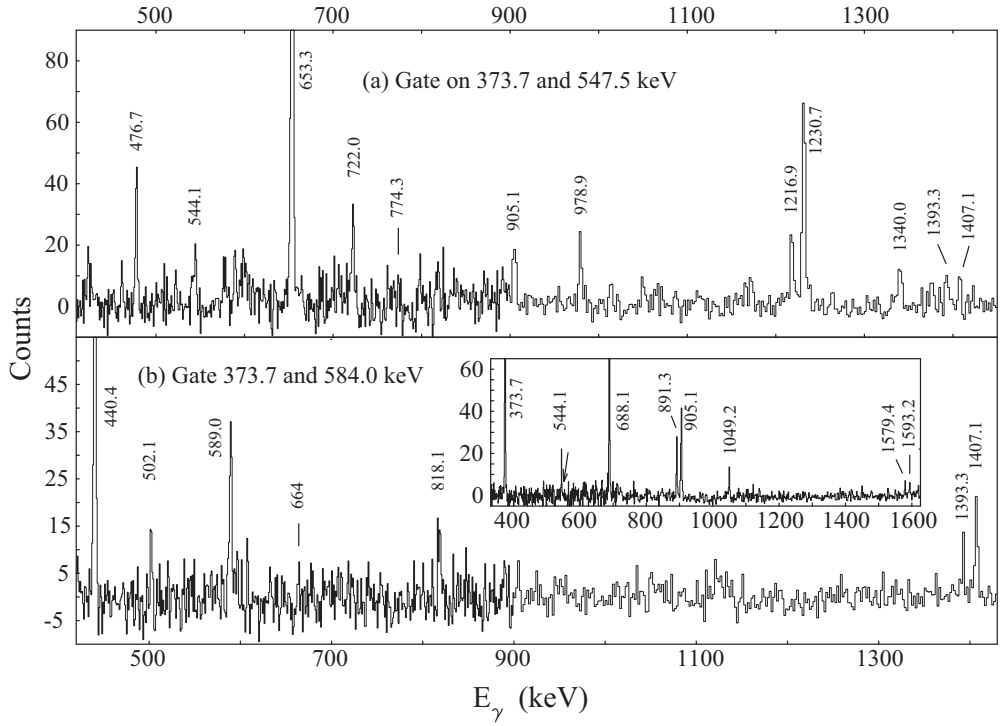

FIG. 7. Coincidence spectra for ^{110}Pd with double gates on (a) 373.7- and 547.5-keV and (b) 373.7- and 584.0-keV γ rays. The inset in (b) shows the spectrum gated on the 440.4- and 397.9-keV transitions. The arrow in the inset shows the expected position of the 547-keV γ ray, previously assigned to the γ band in ^{110}Pd [20].

The relative intensities of γ rays in ^{110}Pd have been determined as described in Sec. II (last paragraph) and presented in Table I. Intensities of some of the weak transitions could not be reliably estimated from spectra with one gate on a complementary fragment γ ray. For example, the intensity of 664-keV transition from the 2651.1-keV state in Band 2 was estimated to be approximately two units based on spectra with gates on ^{110}Pd γ rays only. Also, the relative intensities of several weak transitions from the 1900.1-, 2261.2-, 2791.4-, and 2805.2-keV levels have been determined from previously reported γ-ray branching ratios [24] using the intensities of the relatively stronger transitions from the same level as reference. These are marked with asterisks in Table I.

In addition, transitions at the top of Band 1 were observed to be weak in spectra with one gate on a complementary γ ray. Since states with spin $J^\pi \geqslant (8^+)$ are not fed from β decay, the relative intensities of the transitions from these states in Band 1 with energies 722.0, 774.3, 649.4, and 767.1 keV were estimated from the sum of two double-gated spectra with gates on the (373.7 + 653.3)- and (547.5 + 653.3)-keV transitions where all γ rays belong to ^{110}Pd. These intensities were then normalized with the intensity of the 722.0-keV γ ray obtained from a spectrum with one gate on a complementary fragment γ ray that also gives the intensities of the 547.5- and 653.3-keV transitions in the band.

As stated above, the yrast bands in the neutron-rich Pd isotopes ^{108,112}Pd are crossed by a sequence of transitions above spin 8^+ [21,25]. Similar crossings have been reported in the heavier even-mass Pd isotopes ^{114,116}Pd at rotational frequencies of $\hbar\omega = 0.32$–36 MeV [26]. In the absence of such low-frequency crossing in the neighboring odd Pd isotopes with an unpaired $h_{11/2}$ neutron, as in ^{115}Pd [26], the crossings in the even-A Pd isotopes are attributed to the alignment of pair of neutrons in the $h_{11/2}$ orbital. The unpaired $h_{11/2}$ neutron in the odd-Pd isotopes blocks the low-frequency alignment. The transitions in the aligned band have energies that are very similar to each other, suggesting a mixing of vibrational and rotational motion. Although no such (vibrational) sequence has been reported in ^{110}Pd, the yrast band has been previously observed to be crossed above spin 8^+ by a sequence of two transitions with energies 900 and 522 keV [21]. These two γ rays, in fact, were shown to connect the (8^+) and (10^+) states of the yrast band. However, the 900- and 522-keV transitions were not observed in the present work possibly due to a lack of adequate statistics in the data. It is possible that the yrast band in ^{110}Pd is also crossed by a vibration-like sequence as in the neighboring even-mass Pd isotopes. Further experiments are necessary for testing such possibilities.

In addition, the odd-spin levels in the γ band are known up to 15^+ in ^{114,116}Pd and 13^+ in ^{112}Pd [26]. In contrast, only the (3^+) state is confirmed in the quasi-γ band in ^{110}Pd. The (5^+) state, previously reported to belong to the γ band [21], could not be confirmed in the present work as discussed above. As pointed out in Ref. [26], the degree of even-odd staggering in the γ band indicates whether the nucleus is gamma-soft or if it has a well-developed triaxial shape. Hence, a more detailed study of both Bands 1 and 2 is essential for a clear understanding of the underlying nuclear shapes.

2. *The nucleus* ^{116}Cd

The cadmium isotopes being close to the $Z = 50$ major shell have been considered to be good examples of quadrupole vibrators with spherical shapes [27]. In addition, rotational collectivity has been reported in the neutron-rich Cd isotopes and the study of the evolution of such collectivity with spin and neutron number has been a subject of much interest. A study of the systematics of the energy of the 2^+ states in even-A Cd isotopes suggests that the ground-state yrast band with the probable configuration $\nu h^2_{11/2}$ in ^{116}Cd should be among the most strongly deformed structures in the $Z = 48$ chain. Level lifetimes and reduced transition probabilities $B(E2)$ values in the range 30–110 W.u. have been previously reported in the literature [28] for the 2^+, 4^+, and 6^+ states in the ground-state band in ^{116}Cd. Although the ground state is reported to be axially symmetric, triaxiality is predicted to appear at higher rotational frequencies [29]. The quadrupole deformation β_2 for the 2^+, 4^+, and 6^+ states, deduced from the previous $B(E2)$ values, are found to be between 0.20 and 0.28, assuming a small triaxiality parameter $\gamma = 10°$. This indicates a significant rotational collectivity for the yrast band.

In addition, sequences of states built upon excited 5^- states have also been reported to exhibit rotational collectivity in several even-A neutron-rich Cd isotopes. Such states have been reported up to spin (13^-) in ^{114,120}Cd although states only up to (11^-) are previously observed in ^{116,118}Cd.

The level scheme of ^{116}Cd has been studied previously using deep-inelastic heavy-ion collision [27], the fusion-fission reaction ^{28}Si+ ^{176}Yb [30], and the β decay of the isomeric states of ^{116}Ag [31,32]. While Juutinen *et al.* [27] observed the yrast band up to a spin 10^+, Buforn *et al.* [30] extended the band up to (14^+). However, considerable discrepancy exists in the published level schemes for the sidebands.

The level scheme of ^{116}Cd obtained in the present work is shown in Fig. 6. All states up to 4380.0 keV in the yrast band (Band 1), first reported by Buforn *et al.* [30], have been confirmed in the present work. In addition, a 847.8-keV γ ray has been placed at the top of the band leading to the new level at 5227.8 keV with spin (16^+). States up to 2026.5 keV in the yrast band are also reported to be populated in the β decay of the 127.8-keV isomeric state in ^{116}Ag [32].

The placement of the transitions in Band 1 is supported by the double-gated spectrum shown in Fig. 8(a) with gates on the two lowest transitions in the band having energies 513.3 and 705.9 keV. All low-lying transitions in the band above the 1219.2-keV level, reported previously [30], along with some of the transitions belonging to the sideband (Band 2), are seen in the spectrum. However, the 847.8-keV γ ray is partially masked by the stronger 846.4-keV γ ray from the 2872.9-keV state in Fig. 8(a). The inset in Fig. 8(a) is the sum of two double-gated spectra with gates on (797.9 + 215.2)-keV and (513.3 + 797.9)-keV γ rays. The 847.8-keV γ ray is clearly seen in this spectrum, lending firm support to the placement of the γ ray in the band. Spin assignments for states up to 4380.0 keV are based on earlier work [30]. The spin and parity

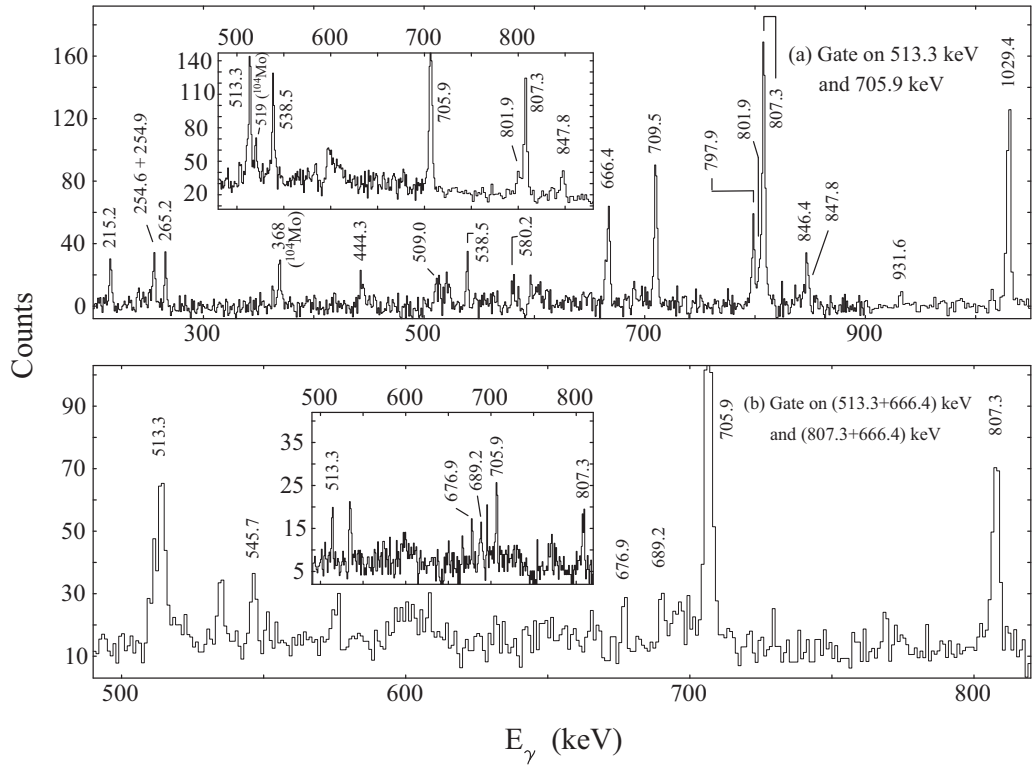

FIG. 8. Double-gated spectra for ^{116}Cd with gates as indicated for (a) and (b). The inset in (a) shows the sum of double-gated spectra with gates on the (797.9 + 215.2)-keV and (513.3 + 797.9)-keV γ rays. The inset in (b) is the spectrum with gates on the 666.4- and 545.7-keV transitions. The 534-keV peak (not marked) in (b) and the inset in (b) is due to a contamination γ ray, possibly belonging to ^{112}Pd.

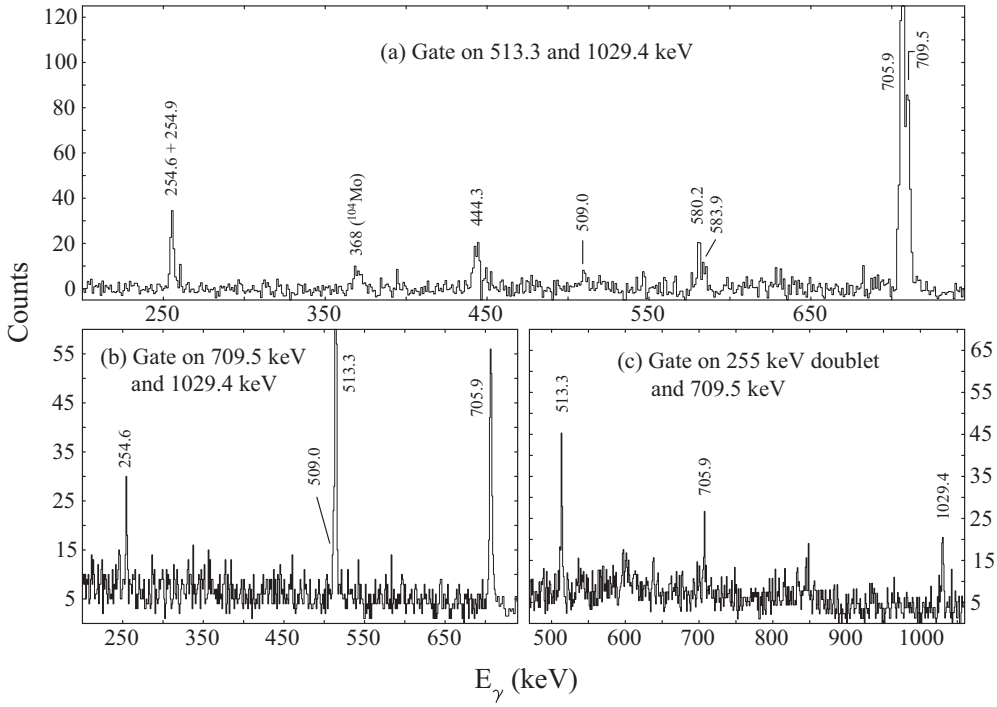

FIG. 9. Double-gated spectra for ^{116}Cd with gates as indicated for (a), (b), and (c). In (c), one of the gates was set on the 255-keV doublet as the individual γ rays could not be resolved.

of the new 5227.8-keV level is tentatively assigned (16^+) based on the systematics within the band.

As already stated, sidebands reported earlier in ^{116}Cd lack consistency. Buforn *et al.* [30] reported a sequence of four states with the 5^- level at 2248.6 keV as the bandhead. The states with spins 5^-, (7^-), (9^-), and (11^-) were observed to be connected by the 444.2-, 689.3-, and 676.9-keV transitions (γ-ray energies as in Fig. 1 in Ref. [30]). However, Batchelder *et al.* [31] have reported only the 444-keV transition connecting the two lowest-energy states in this sequence. In fact, the latter have also reported the non-observation of the 689.3- and 676.9-keV transitions above the (7^-) state in this band. Juutinen *et al.* [27] did not report any of these states. Instead, they reported a band built upon an excited 0^+ state, interpreted as a two quadrupole-phonon state in the vibrator picture, with links to the yrast band. All transitions assigned to this band were observed to be very weak with intensities that are about two to four orders of magnitude less than the $4^+ \rightarrow 2^+$, 705.9-keV transition in the yrast band (see Fig. 3 in Ref. [27]). Subsequently, most of the states belonging to this band were also observed in the β decay of the isomeric states of ^{116}Ag [31,32].

In the present work, a sideband with a sequence of five states, built upon the previously reported 5^-, 2248.6-keV state (Band 2 in Fig. 6), is proposed to replace the sequence of four states reported earlier by Buforn *et al.* [30]. The new transition in this sequence is the one with energy 545.7 keV which is placed above the (7^-) state. With the 676.9- and 689.2-keV γ rays, earlier reported by Buforn *et al.* [30], placed above the 545.7-keV transition, the sequence extends up to an excitation energy of 4604.7 keV and a tentative spin of (13^-). The 3238.6-, 3915.5-, and 4604.7-keV levels in Band 2 are new. It may be noted that the ordering of the 676.9- and 689.2-keV transitions in the level scheme is reversed compared to their placements in Ref. [28]. This is done on the basis of the relative intensities of the two γ rays (Table II). These placements, including that of the new 545.7-keV γ ray, are supported by the double-gated spectra shown in Fig. 8(b) and the inset therein. The spectrum in Fig. 8(b) is the sum of two double-gated spectra with gates on (513.3 + 666.4) keV and (807.3 + 666.4) keV and shows all three transitions in the band above the (7^-) state. The inset shows the spectrum gated on the new 545.7-keV transition and the 666.4-keV γ ray. Observation of the 676.9- and 689.2-keV γ rays belonging to Band 2 and the three low-lying transitions of Band 1 in this spectrum lends a firm support to the placement of the new 545.7-keV transition.

In addition to the band built on the 5^- state, two new states with energies 3212.7 and 3721.7 keV, the latter tentatively, are proposed to be placed above the 2958.1-keV level in ^{116}Cd. States somewhat similar to these have also been reported earlier in ^{118}Cd [29]. The 2958.1-keV level is reported previously from β-decay studies only [31,32]. It is established in the present work primarily on the basis of the observation of the 709.5-keV γ ray. The other two transitions from this level with energies 265.2 and 931.6 keV were found to be very weak, considering fission decays only (Table II). The large intensity of these two γ rays and the 709.5-keV γ ray in the spectrum in Fig. 8(a) is due to contributions from both fission as well as β decay, with the latter being the major contributor.

The two new states at 3212.7- and 3721.7-keV decay by the 254.6- and 509.0-keV transitions, respectively (Fig. 6). The 254.6- and the 254.9-keV γ rays, the latter deexciting the

2503.5-keV state, form a doublet (Fig. 6). The 2503.5-keV state has been previously reported only from β-decay studies. The spectrum in Fig. 9(a) shows both components of the 255-keV doublet as well as the new 509.0-keV γ ray.

The spectra in Figs. 9(b) and 9(c) provide clear evidence for the placement of the 254.6-keV transition above the 2958.1-keV state. Of the 255-keV doublet, the spectrum in Fig. 9(b) with gates on the 709.5- and 1029.4-keV transitions shows a 254.6-keV γ ray. This γ ray cannot be the one that is reported previously to de-excite the 2503.5 keV level from β-decay studies unless there is a significant contribution from the 705.9-keV γ ray in the 709.5-keV gate (see Fig. 6). As this would lead to observation of the 709.5-keV γ ray in the spectrum, of which there is no significant evidence, it would be reasonable to place the 254.6-keV γ ray above the 2958.1-keV state as shown in Fig. 6. The spectrum in Fig. 9(c) with gates on the 255-keV doublet and the 709.5-keV transition shows the 705.9-keV γ ray as expected. The 254.6-keV γ ray is possibly due to prompt fission events only as the 3212.7-keV level has not been reported from β-decay studies so far. Evidence in favor of placement of the 509.0-keV transition at the top of Band 2 is mainly provided in Fig. 9(a). The 509.0-keV peak in Fig. 9(b) suffers from being masked by the stronger 513.3-keV γ ray. The present data only permit a tentative placement of the 509.0-keV γ ray above the 3212.7-keV level.

Relative intensities of most of the γ rays (see Table II), including those near the top of Band 1, were determined following the procedure outlined in Sec. II (last paragraph). The present branching ratios for the 444.3- and 666.4-keV transitions from the 2692.9-keV state and the 166.7- and 215.2-keV transitions from the 3039.6-keV level are in agreement within experimental errors with published results [31,33]. Among the weak transitions, the relative intensities of the 265.2- and 931.6-keV γ rays were estimated from their branching ratios with respect to the strong 709.5-keV γ ray obtained from the spectrum gated by the 513.3- and 705.9-keV transitions [spectrum in Fig. 8(a)] belonging to ^{116}Cd. The intensity of the 509.0-keV γ ray, supposedly having no contribution from β decay, was also estimated from the same spectrum and normalized to that of the 538.5-keV transition. However, only an approximate value is adopted (in Table II) in view of the somewhat large error involved in this exercise.

The yrast band in ^{116}Cd, with a significant rotational collectivity, shows a sharp back-bending at a rotational frequency of $\hbar\omega \sim 0.4$ MeV due to the quasirotational alignment of a pair of $h_{11/2}$ neutrons. This is supported by Nilsson cranked shell-model calculations that also predict the $\pi p^2_{1/2}$ crossing at $\sim$0.65 MeV [29]. Although the band has been extended up to spin (16^+) in the present work, the latter prediction can only be experimentally verified by extending the band to still higher spins.

It may be noted that the sideband reported by Buforn *et al.* [30] in neighboring ^{114}Cd is also built upon a 5^- state and extends up to spin (13^-). The level energies of the sidebands in ^{114}Cd and ^{116}Cd bear a remarkable resemblance to each other and indicate a similarity in their structure. These bands have been interpreted as having the two-quasiparticle configuration $\nu h_{11/2} \otimes \nu g_{7/2}$. Bands with the 5^- state as the bandhead have also been reported in ^{118}Cd up to a spin of (11^-) and in ^{120}Cd up to (13^-) [29]. The 5^- levels in ^{118,120}Cd, as well as in some of the lighter Cd isotopes, have also been interpreted as possible candidates of quadrupole-octupole phonon coupled $2^+ \otimes 3^-$ states [29].

IV. CONCLUSION

Prompt γ-ray spectroscopy of primary fission fragments produced in the reaction ^{208}Pb(^{18}O,f) at $E = 90$ MeV has been performed. Fission fragment isotopic distributions have been determined for 12 even-Z, even-N fragments and the fission-fragment mass distribution derived from the sum of the yields of the individual nuclei have been studied. The relative yields of both odd- and even-A isotopes of Mo, Ru, Pd, and Cd and the isotones of $N = 62$, 64 have been measured to study the odd-even effects associated with the fission process. The odd-even effect in neutron number is observed to be more pronounced than the odd-even effect in proton number. The large yields of ^{103}Mo and ^{105}Tc may be attributed to structural effects. The average total neutron multiplicity, pertaining to both pre- and postscission neutrons, has been found to be 5.48 $\pm$ 0.59. Considering that the prescission neutron number is about 3, a postscission neutron multiplicity of 2.5 is expected to correspond to a moderate deformation of the fragments at scission.

The level schemes of two neutron-rich nuclei ^{110}Pd and ^{116}Cd have been studied from $\gamma\gamma\gamma$ coincidences. Several transitions, previously reported only from β-decay studies, have been assigned to ^{110}Pd from prompt fission decay. The yrast band in ^{116}Cd has been extended up to an excitation energy of 5227.8 keV and spin (16^+). In addition, the sideband built upon the excited 5^- state has been observed up to spin (13^-) for the first time. The band was previously reported up to (11^-). Results for the two nuclei ^{110}Pd and ^{116}Cd have been discussed in the context of earlier experimental observations and theoretical calculations.

ACKNOWLEDGMENTS

The first author (P.B.) gratefully acknowledges the financial support provided by Council of Scientific and Industrial Research (CSIR), Human Resource Development Group, vide Project No. 21(0943)/12/EMR-II for the Emeritus Scientist scheme. The authors thank the Indian National Gamma Array collaboration for setting up the array of clover detectors at the BARC-TIFR Pelletron LINAC facility at the Tata Institute of Fundamental Research (TIFR), Mumbai, India. They also thank the staff of the Target Laboratory at TIFR for providing the necessary help and facilities for the preparation of the target. The assistance provided by Mr. Pradipta Das of Saha Institute of Nuclear Physics in target preparation and the Pelletron operating staff in the operation of the Pellletron is sincerely acknowledged. One of the authors (S.G.) acknowledges the financial support provided by the UGC-DAE-CSR-KC vide Project No. UGC-DAE-CSR-KC/CRS/13/NP06/.

[1] J. B. Wilhelmy, E. Cheifetz, R. C. Zared, S. G. Thompson, H. R. Bowman, and J. O. Rasmussen, Phys. Rev. C **5**, 2041 (1972).

[2] R. P. Schmitt, G. Mouchaty, and D. R. Haenni, Nucl. Phys. A **427**, 614 (1984).

[3] L. S. Danu, D. C. Biswas, A. Saxena, A. Shrivastava, A. Chatterjee, B. K. Nayak, R. G. Thomas, R. K. Choudhury, R. Palit, I. Mazumdar, P. Datta, S. Chattopadhyay, S. Pal, S. Bhattacharya, S. Muralithar, K. S. Golda, R. K. Bhowmik, J. J. Das, R. P. Singh, N. Madhavan, J. Gerl, S. K. Patra, and L. Satpathy, Phys. Rev. C **81**, 014311 (2010).

[4] A. Bogachev, L. Krupa, O. Dorvaux, E. Kozulin, M. Itkis, M.-G. Porquet, A. Astier, D. Curien, I. Deloncle, G. Duchene, B. J. P. Gall, F. Hanappe, F. Khalfallah, M. Rousseau, L. Stuttge, N. Redon, and O. Stezowski, Eur. Phys. J. A **34**, 23 (2007).

[5] J. H. Hamilton, A. V. Ramayya, S. J. Zhu, G. M. Ter-Akopian, Yu. Ts. Oganessian, J. D. Cole, J. O. Rasmussen, and M. A. Stoyer, Prog. Part. Nucl. Phys. **35**, 635 (1995).

[6] X. Q. Zhang, J. H. Hamilton, A. V. Ramayya, S. J. Zhu, J. K. Hwang, C. J. Beyer, J. Kormicki, E. F. Jones, P. M. Gore, B. R. S. Babu, T. N. Ginter, R. Aryaeinejad, K. Buttler-Moore, J. D. Cole, M. W. Drigert, J. K. Jewell, E. L. Reber, J. Gilat, I. Y. Lee, J. O. Rasmussen, A. V. Daniel, Y. T. Oganessian, G. M. Ter-Akopian, W. C. Ma, P. G. Varmette, L. A. Bernstein, R. W. Lougheed, K. J. Moody, M. A. Stoyer, R. Donangelo, and J.-Y. Zhang, Phys. Rev. C **63**, 027302 (2001).

[7] A. Astier, M.-G. Porquet, Ts. Venkova, Ch. Theisen, G. Duchene, F. Azaiez, G. Barreau, D. Curien, I. Deloncle, O. Dorvaux, B. J. P. Gall, M. Houry, R. Lucas, N. Redon, M. Rousseau, and O. Stézowski, Eur. Phys. J. A **50**, 2 (2014).

[8] R. Palit, S. Saha, J. Sethi, T. Trivedi, S. Sharma, B. S. Naidu, S. Jadhav, R. Donthi, P. V. Chavan, H. Tan, and W. Hennig, Nucl. Instrum. Methods A **680**, 90 (2012).

[9] D. C. Radford, Nucl. Instr, Meth. Phys. Res. A **361**, 297 (1995).

[10] H. Seyfarth, H. H. Güven, B. Kardon, W. D. Lauppe, G. Lhersonneau, K. Sistemich, S. Brant, N. Kaffrell, P. Maier-Komor, H. K. Vonach, V. Paar, D. Vorkapić, and R. A. Mayer, Z. Phys. A **339**, 269 (1991).

[11] A. D. Yamamoto, Ph.D. thesis, University of Surrey, 2004.

[12] D. de Frenne and E. Jacobs, Nucl. Data Sheets **105**, 775 (2005).

[13] N. Fotiades, J. A. Cizewski, D. P. McNabb, K. Y. Ding, D. E. Archer, J. A. Becker, L. A. Bernstein, K. Hauschild, W. Younes, R. M. Clark, P. Fallon, I. Y. Lee, A. O. Macchiavelli, and R. W. MacLeod, Phys. Rev. C **58**, 1997 (1998).

[14] H. Mach, F. K. Wohn, G. Molnár, K. Sistemich, John C. Hill, M. Moszynski, R. L. Gill, W. Krips, and D. S. Brenner, Nucl. Phys. A **523**, 197 (1991).

[15] M. Liang, H. Ohm, I. Ragnarsson, and K. Sistemich, Z. Phys. A **346**, 101 (1993).

[16] Y. X. Luo, J. O. Rasmussen, J. H. Hamilton, A. V. Ramayya, J. K. Hwang, S. J. Zhu, P. M. Gore, S. C. Wu, I. Y. Lee, P. Fallon, T. N. Ginter, G. M. Ter-Akopian, A. V. Daniel, M. A. Stoyer, R. Donangelo, and A. Gelberg, Phys. Rev. C **70**, 044310 (2004).

[17] L. M. Pant, A. Saxena, R. G. Thomas, D. C. Biswas, and R. K. Choudhury, Eur. Phys. J. A **16**, 43 (2003).

[18] J. F. Wild, J. van Aarle, W. Westmeier, R. W. Lougheed, E. K. Hulet, K. J. Moody, R. J. Dougan, E.-A. Koop, R. E. Glaser, R. Brandt, and P. Patzelt, Phys. Rev. C **41**, 640 (1990).

[19] Y. Wang, P. Dendooven, J. Huikari, A. Jokinen, V. S. Kolhinen, G. Lhersonneau, A. Nieminen, S. Nummela, H. Penttilä, K. Peräjärvi, S. Rinta-Antila, J. Szerypo, J. C. Wang, and J. Äystö, Phys. Rev. C **63**, 024309 (2001).

[20] M. Houry, R. Lucas, M.-G. Porquet, Ch. Theisen, M. Girod, M. Aiche, M. M. Aleonard, A. Astier, G. Barreau, F. Becker, J. F. Chemin, I. Deloncle, T. P. Doan, J. L. Durell, K. Hauschild, W. Korten, Y. Le Coz, M. J. Leddy, S. Perries, N. Redon, A. A. Roach, J. N. Scheurer, A. G. Smith, and B. J. Varley, Eur. Phys. J. A **6**, 43 (1999).

[21] S. Lalkovski, A. Minkova, M.-G. Porquet, A. Bauchet, I. Deloncle, A. Astier, N. Buforn, L. Donadille, O. Dorvaux, B. P. J. Gall, R. Lucas, M. Meyer, A. Prévost, N. Redon, N. Schulz, and O. Stézowski, Eur. Phys. J. A **18**, 589 (2003).

[22] J. äystö, C. N. Davids, J. Hattula, J. Honkanen, K. Honkanen, P. Jauho, R. Julin, S. Juutinen, J. Kumpulainen, T. Lönnroth, A. Pakkanen, A. Passoja, H. Penttilä, P. Taskinen, E. Verho, A. Virtanen, and M. Yoshii, Nucl. Phys. A **480**, 104 (1988).

[23] G. Lhersonneau, J. C. Wang, S. Hankonen, P. Dendooven, P. Jones, R. Julin, and J. Äystö, Phys. Rev. C **60**, 014315 (1999).

[24] G. Gürdal and F. G. Kondev, Nucl. Data Sheets **113**, 1315 (2012).

[25] R. Krücken, S. J. Asztalos, R. M. Clark, M. A. Deleplanque, R. M. Diamond, P. Fallon, I. Y. Lee, A. O. Macchiavelli, G. J. Schmid, F. S. Stephens, K. Vetter, and Jing-Ye Zhang, Eur. Phys. J. A **10**, 151 (2001).

[26] Y. X. Luo, J. O. Rasmussen, J. H. Hamilton, A. V. Ramayya, S. Frauendorf, J. K. Hwang, N. J. Stone, S. J. Zhu, N. T. Brewer, E. Wang, I. Y. Lee, S. H. Liu, G. M. TeraAkopian, A. V. Daniel, Y. T. Oganessian, M. A. Stoyer, R. Donangelo, W. C. Ma, J. D. Cole, Yue Shi, and F. R. Xu, Nucl. Phys. A **919**, 67 (2013).

[27] S. Jutinen, R. Julin, P. Jones, A. Lampinen, G. Lhersonneua, E. Mäkelä, M. Piiparinen, A. Savelius, and S. Törmänen, Phys. Lett. B **386**, 80 (1996).

[28] M. Kadi, M. Warr, P. E. Garrett, J. Jolie, and S. W. Yates, Phys. Rev. C **68**, 031306(R) (2003).

[29] Y. X. Luo, J. A. Rasmussen, C. S. Nelson, J. H. Hamilton, A. V. Ramayya, J. K. Hwang, S. H. Liu, C. Goodin, N. J. Stone, S. J. Zhu, N. T. Brewer, Ke Li, I. Y. Lee, G. M. Ter-Akopian, A. V. Daniel, M. A. Stoyer, R. Donangelo, W. C. Ma, and J. D. Cole, Nucl. Phys. A **874**, 32 (2012).

[30] N. Buforn, A. Astier, J. Meyer, M. Meyer, S. Perriès, N. Redon, O. Stézowski, M. G. Porquet, I. Deloncle, A. Bauchet, J. Duprat, B. J. P. Gall, C. Gautherin, E. Gueorguieva, F. Hoellinger, T. Kutsarova, R. Lucas, A. Minkova, N. Schulz, H. Sergolle, Ts. Venkova, and A. N. Wilson, Eur. Phys. J. A **7**, 347 (2000).

[31] J. C. Batchelder, J.-C. Bilheux, C. R. Bingham, H. K. Carter, D. Fong, P. E. Garrett, R. Grzywacz, J. H. Hamilton, D. J. Hartley, J. K. Hwang, W. Krolas, W. D. Kulp, Y. Larochelle, A. Piechaczek, A. V. Ramayya, K. P. Rykaczewski, E. H. Spejewski, D. W. Stracener, M. N. Tantawy, J. A. Winger, J. L. Wood, and E. F. Zganjar, Phys. Rev. C **72**, 044306 (2005).

[32] J. C. Batchelder, J. L. Wood, P. E. Garrett, K. L. Green, K. P. Rykaczewski, J.-C. Bilheux, C. R. Bingham, H. K. Carter, D. Fong, R. Grzywacz, J. H. Hamilton, D. J. Hartley, J. K. Hwang, W. Krolas, W. D. Kulp, Y. Larochelle, A. Piechaczek, A. V. Ramayya, E. H. Spejewski, D. W. Stracener, M. N. Tantawy, J. A. Winger, and E. F. Zganjar, Phys. Rev. C **80**, 054318 (2009).

[33] Jean Blachot, Nucl. Data Sheets **111**, 738 (2010).